Rapid fabrication of high density C/C composite by coupling of processes

T. S. K. Raunija[1,2*], R. K. Gautam[2], S.C. Sharma[3], A. Verma[2*]

[1]*Carbon and Ceramics Laboratory (CCL), Materials and Mechanical Entity, Vikram Sarabhai Space Centre, Indian Space Research Organisation, Thiruvananthapuram 695022, Kerala, India*
[2]*Sustainable Environergy Research Lab (SERL), Department of Chemical Engineering, Indian Institute of Technology Delhi, Hauz-Khas 110016, New Delhi, India*
[3]*Materials and Metallurgy Group (MMG), Materials and Mechanical Entity, Vikram Sarabhai Space Centre, Indian Space Research Organisation, Thiruvananthapuram 695022, Kerala, India*

*Corresponding author: E-mail: thakurskr@gmail.com; anilverma@iitd.ac.in

Abstract

The main objective of the work was to rapidly prepare high density short carbon fiber reinforced randomly oriented C/C composite by coupling the processes. The C/C composite was fabricated by coupling two processes. In primary high pressure HP method, medium density C/C composite was prepared by mixing the exfoliated carbon fibers and PMP with distilled water; moulding of the slurry; drying of the green cake; hot-pressing of the preform and finally carbonizing the compact. In secondary low pressure ITC method, the medium density C/C composite was densified by SMP in three repeated cycles to obtain high density. The composite was characterized for microstructure, density, porosity, hardness, flexural strength, compressive strength and permeability. The results showed that the coupling of primary method with secondary method resulted in fine microstructure, high density (1.70 g/cm^3), excellent mechanical properties (flexural strength 77 MPa and compressive strength 161 MPa) and reduced porosity & permeability. Copyright © 2016 VBRI Press.

Keywords: Exfoliation; mixing; moulding; hot-pressing; carbonization; densification; coupling; C/C composite.

Introduction

Carbon/carbon (C/C) composite since its first successful synthesis in 1970s [1] has been extensively studied. It is the composite which is comprised of carbon as reinforcement and derived carbon as matrix. In the fabrication of C/C composite; various types and forms of carbon reinforcement are used for reinforcing whereas various resins, pitches and hydrocarbon gases are used to derive carbon matrix [2-8]. It possess wide spectrum of properties depending upon the combination of reinforcement and matrix precursors used for its fabrication [9]. Due to wide spectrum of properties, it is used in variety of applications like air-craft brake disk [10-11], turbine disk for the air turbo ramjet engine [12], cages for rolling element bearing [13], rocket nozzles [14-15], solid rocket motor vanes [16-17], heat sinks [18], reciprocating components of intermittent combustion engines [19], and nuclear reactor plasma components [20-21]. In addition to this, C/C composite possess all the essential properties required for using it as a bipolar plate of PEM fuel cell and researchers [22] have successfully demonstrated its usage for the same. However, the processing time, cost and permeability are the major issues hindering its commercial usage for bipolar plate.

Over the past years, several types of C/C composite including whisker, particulate and fiber reinforced have been studied extensively. However, much attention has been focused on continuous carbon fiber reinforced C/C composite. In contrast to continuous fiber reinforced composites, short fiber reinforced composites have emerged as rapid and cost effective. Due to these advantages, in last couple of years, they have attracted the attention of the designers and researchers [17, 23]. Even, some researchers have tried to reduce the cost of C/C composite by the usage of short carbon fibers as reinforcement [24-27] and derivation of carbon matrix from high carbon yield pitch based matrix precursors [28]. The reason behind the usage of such matrix precursors is to limit the densification cycles and hence, reducing the time and cost of fabrication [29]. Even, we have demonstrated viability of making low cost C/C composite through high pressure hot-pressing (HP) method in a record time of 90 h [30]. However, high pressure HP method alone couldn't give a C/C system best suitable for bipolar plate application. More specifically, the permeability of the composite was on higher side restricting its use for said applications. Hence, further work to make it suitable for the application by patching up these issues need to be done. Accordingly, we took up the present work. The C/C composite obtained in high pressure HP method [30] was subjected to secondary low pressure impregnation-thermosetting-carbonization

(ITC) method for improving the density & mechanical properties and reducing the porosity & permeability. Further, impact of hot-pressing heating rate in wide range on the densification behavior was studied. Additionally, several new denominations for commercial viability assessment of composite system were derived and their relevance was discussed.

Experimental

Materials and methods

The as received continuous carbon fiber spools of high modulus & high conductivity pitch based P-75 grade (BP Amoco Thornel, USA) and high strength PAN based T-800 grade (Toray Industries Inc, Japan) were fed to fiber milling machine to obtain discrete length carbon fibers. The details about producing discrete length carbon fibers were reported earlier [31]. The discrete length carbon fibers were exfoliated using the methodology reported earlier [29]. The exfoliated carbon fibers were then used as reinforcement. As received commercial petroleum pitch was converted into isroaniso matrix precursor (IMP) at Carbon and Ceramics Laboratory of Vikram Sarabhai Space Centre (VSSC) through in-house developed process technology. The IMP is a specially synthesized mesophase pitch best suitable as a matrix precursor for deriving carbon matrix. The IMP after air stabilization (named as SP) was used as primary matrix precursor (PMP) for deriving primary carbon matrix (PCM). The in-house synthesized resole type phenolic resin (PF 106 grade, produced at PFC/VSSC) was used as secondary matrix precursor (SMP) for deriving secondary carbon matrix (SCM). Distilled water produced in-house using double distillation column was used as slurry media for preparing the slurry of reinforcement and PMP. High purity argon gas received from Bhuruka Gases Limited, Bengaluru was used for maintaining inert atmosphere at high temperatures to avoid oxidation of the compacts.

Compact preparation

C/C composite was prepared by coupling two methods; high pressure HP method and low pressure ITC method. In primary method, medium density C/C composite was prepared by using exfoliated carbon fibers and PMP. Medium density C/C composite thus obtained was densified in secondary method using SMP. The step by step details of both the methods to obtain high density C/C composite are described in subsequent sections.

High pressure HP method

High pressure HP method is the novel method developed at Carbon and Ceramics Laboratory of Vikram Sarabhai Space Centre for making medium density C/C composite [29-30]. The details about each step of high pressure HP method are described in subsequent sections.

Mixing

The exfoliated carbon fibers and PMP were well mixed in distilled water by agitating the ingredients vigorously in the mixing and moulding set-up to obtain well-mixed slurry. The specially designed sharp and flat blades in combination were used during mixing to split and uniformly disperse reinforcement in PMP and distilled water. The mixing was carried out at 120 rpm for 60 min.

Moulding

The well-mixed slurry was moulded in rectangular cross-section (70 mm x 50 mm) metallic die. The moulding was carried out in the mixing-moulding set-up under continuous vacuum and pulsed form of mild pressure to obtain green cake.

Drying

Though most of the distilled water used for making green cake was squeezed out during moulding, the remaining distilled water was removed by drying the green cake along with metallic die in an electric air oven at moderate temperature to obtain preform.

Hot-pressing

The dry preform along with metallic die was loaded on a indigenously developed medium pressure hot-press. The hot-pressing is the key step of primary method. During hot-pressing, PMP melts and flows in between carbon fiber filaments to bind them following by polymerization, condensation and cyclization reactions. The hot-pressing was carried out at 650°C under 15 MPa pressure. Total six compacts were prepared by varying hot-pressing rate from 3.3 to 0.1°C/min. The compacts were designated as $HR_{3.3}$, $HR_{1.0}$, $HR_{0.5}$, $HR_{0.3}$, $HR_{0.2}$ and $HR_{0.1}$ for 3.3, 1.0, 0.5, 0.3, 0.2 and 0.1°C/min, respectively.

Low pressure ITC method

The medium density C/C composite obtained through high pressure HP method were densified through three repeated cycles of low pressure ITC method. The first cycle was named as DC1, second cycle as DC2 and third cycle as DC3. The details about each step of low pressure ITC method are described in subsequent sections.

Pore evacuation

Pore evacuation is the first step of low pressure ITC method and in this all the C/C compacts, were subjected to pore evacuation under the application of vacuum. In this mainly, the air filled in the pores is removed so that SMP can infiltrate more effectively to the core of the compact.

Resin infiltration

Subsequent to pore evacuation, the SMP was poured under vacuum and allowed to fill the pores. The deep penetration of the SMP into fine and deep pores was achieved by the application of low pressure. The air pressure of 7 bar was applied for 3 h to push the SMP into fine pores. The usage of 7 bar and 3 h pressure and time, respectively was done based on the optimum value of pressure and time w.r.t. cost and time of processing [32]. Both pore evacuation and resin impregnation were carried out in single resin-impregnation unit.

Thermosetting

The SMP filled compacts were taken out from the resin-impregnation set-up and wiped out for the extra resin available on the surface. The compacts were then kept in an oven at 220°C and allowed to thermoset the infiltrated SMP within the pores.

Carbonization

The impregnated-thermoset compacts were carbonized in a Thermosystem make tubular furnace. The carbonization was carried @ 1°C/min upto 1050°C and soaking at maximum temperature was carried out for 60 min. The rapid cooling was achieved by the usage of specially designed carbonization furnace. Inert atmosphere was maintained by purging argon gas inside the hot-zone @ 5 L/min.

Characterization

Morphology

Carl Zeiss make, SMT EVO 50 model, scanning electron microscope (SEM) and Carl Zeiss make, SIGMA HD model, field emission scanning electron microscope (FESEM) were used for examining the surface morphology of the compacts. SEM images of the compacts were taken after primary method and three point bending test. The microstructure analysis of the compacts after secondary method was done using FESEM.

Density

Bulk density of the compacts was measured by mass-volume formula. The equation used is described below:

$$\rho_b = \frac{m}{V} \tag{1}$$

where

ρ_b = bulk density,

m = mass,

V = volume.

The bulk density of the compacts was experimentally measured after hot-pressing (H) and carbonization (C) stages of primary method and each complete cycle (DC1, DC2 and DC3) of secondary method. The theoretical density of the compacts after primary method was computed as follows:

$$\rho_{tc} = v_r\rho_r + v_{pcm}\rho_{pcm} \tag{2}$$

where,

ρ_{tc} = theortical density of the compact after primary method,

v_r = volume fraction of reinforcement in the compact after primary method,

ρ_r = density of reinforcement,

v_{pcm} = volume fraction of PCM in the compact after primary method,

ρ_{pcm} = possible density of PCM obtained from PMP after primary method.

The density of the reinforcement was taken as such from the supplier's data sheet for computing the aforementioned theoretical density. Though Rellick [33] had reported the densification of carbon fibers during processing (graphitization), the same influence on carbon fibers was not considered in our calculations because we haven't graphitized the compacts. Further, the density of PCM and the volume fractions of reinforcement and PCM after high pressure HP method were assumed and calculated, respectively. The density of PCM was assumed based on the literature inputs available for carbon matrix derived from similar matrix precursors. The density of the carbon matrix derived from pitch after graphitization was taken between 2.18-2.25 g/cm^3 by Rellick [33]. Since we haven't graphitized the compacts like Rellick [33], the assumption of the density between 2.18-2.25 g/cm^3 might not be correct for all the calculations. Hence, a density of 1.95 g/cm^3 was considered for the carbon matrix derived from PMP during high pressure HP method. This is slightly higher than that reported by Matzinos *et al.* [34] for pitch coke. This assumption was done by considering the fact that the PMP because of liquid crystals may result in higher density carbon matrix after carbonization than normal pitch matrix precursor which was used by Matzinos et al. [34]. Further, the volume fractions of reinforcement and matrix in the compact after high pressure HP method were calculated as follows:

$$v_r = \frac{U_r}{U_r + U_{pcm}} \tag{3}$$

$$v_{pcm} = \frac{U_{pcm}}{U_{pcm} + U_r} \tag{4}$$

where

U_r = volume of reinforcement after high pressure HP method,

U_{pcm} = volume of PCM derived from PMP during high pressure HP method.

Since the volume of reinforcement and matrix in the compact after high pressure HP method can't be calculated directly through experimental means, it was computed indirectly by knowing the weight and density of the constituents. The density of the reinforcement was known from supplier's data sheet and that of matrix was assumed as 1.95 g/cm^3. The weight of the PCM remaining in the compact after high pressure HP method was calculated by knowing the weight loss of PMP during processing and carbon yield of the PMP during high pressure HP method. Further, the weight of the reinforcement remaining in the compact after high pressure HP method was calculated by deducting the weight loss of carbon fibers at carbonization temperature from that of initial taken. The detailed calculation methodology can be understood with the help of following equations:

$$U_{pcm} = \frac{w_{pcm}}{\rho_{pcm}} \tag{5}$$

$$U_r = \frac{w_{rc}}{\rho_r} \tag{6}$$

$$w_{pcm} = (w_{pmpi} - w_{pmpp}) \times y_{HP} \tag{7}$$

$$w_{rc} = (w_{ri} - w_{rp}) \tag{8}$$

where,

w_{pcm} = weight of PCM in compact after high pressure HP method,

w_{rc} = weight of reinforcement in compact after high pressure HP method,

w_{pmpi} = weight of PMP taken initially,

w_{pmpp} = weight loss of PMP during processing,

w_{ri} = weight of reinforcement taken initially,

w_{rp} = weight loss of reinforcement during processing,

y_{HP} = carbon yield of PMP during high pressure HP method.

Determination of densification efficiency

The densification efficiency, more specifically the volumetric densification efficiency was first defined by Rellick [33] as the ratio of the volume of the pitch coke formed to the void volume before treatment. This is the most useful parameter defined so far for the assessment of the efficiency of the densification. The equation is given below:

$$y_v = y_{ITC} Y_l \frac{\rho_{smp}}{\rho_{scm}} \qquad (9)$$

where,

y_v = volumetric densification efficiency

y_{ITC} = carbon yield of the SMP

Y_l = overall SMP impregnation efficiency

ρ_{smp} = density of SMP

ρ_{scm} = density of SCM obtained from SMP

Using the above relationship, the maximum densification efficiency per cycle can be estimated. Taking $y_{ITC} = 55\%$ as an upper limit for phenolic resin, $\rho_{smp} = 1.3 \text{ g/cm}^3$, $\rho_{scm} = 1.8 \text{ g/cm}^3$ and assuming perfect liquid impregnation efficiency ($Y_l = 1$), the maximum densification efficiency per cycle can be estimated from Equation 11 to be $y_v = 0.397$.

Porosity determination from density measurement

Since the C/C composite made in accordance with the present methodology (high pressure HP method) adopted by us doesn't have any preform density like those of 2-D, 3-D preforms, the density after high pressure HP method was taken as the baseline for the determination of effective porosity. The porosity was calculated as follows:

$$\theta_{HP} = (\rho_{tc} - \rho_{bHP}) \qquad (10)$$

where

θ_{HP} = porosity of the compact after high pressure HP method,

ρ_{bHP} = bulk density of the compact after high pressure HP method.

The porosity computed in accordance with the equation given above was total porosity whereas Matzinos et al. [34] has used open porosity in their calculations of densification efficiency. Since the close porosity may

become open during repeated densification cycles as a result of cyclic thermal stresses, the calculations by considering only open porosity may not be correct. Hence, we have considered total porosity for our calculations. Further, the theoretical porosity of the compacts after each densification cycle was worked out using the following equation [33],

$$\theta_{tn} = \theta_{HP}(1 - y_v)^n \qquad (11)$$

where

θ_{tn} = theortical porosity of the compact after n^{th} ITC cycle,

n = numberof ITC cycles

The actual porosity of the compacts after each densification cycle was determined by the following equation:

$$\theta_{an} = (\rho_{tc} - \rho_{bnITC}) \qquad (12)$$

where

θ_{an} = actual porosity of the compact after n^{th} cycle,

ρ_{bnITC} = bulk density of the compact after n^{th} ITC cycle.

Mechanical properties

Both flexural and compressive strengths were measured using universal testing machine (Instron 5500R standard). Flexural strength was evaluated as per ASTM C1161-02C whereas compressive strength was tested as per ASTM C695-91(Reapproved 2005). The optimum dimensions of test specimens for flexural test and compressive test were taken as 3 mm x 4 mm x 45 mm and 9 mm x 9 mm x 18 mm, respectively. Both compressive and flexural strengths were tested in in-plane direction only. An average of five specimens was reported.

Surface hardness of C/C composite samples was measured by means of a Barcol impressor (Barber Colman GYZJ-934-1 standard). Barcol hardness test characterizes the indentation hardness of materials through the depth of penetration of an indentor loaded on a material sample and compared to the penetration in a reference material. The governing standard for Barcol hardness test is ASTM D2583. Barcol hardness is measured on a scale from 0 to 100 with the typical range between 30 and 90 B. A measurement of 60 B is roughly equivalent to Shore hardness of 80 D or Rockwell hardness of M100. As defined in ASTM D2583, each scale division from 0-100 should indicate a depth of 0.0076 mm. The Barcol hardness of the compacts was measured after primary method and secondary method. Total six indentations on each compact were made and an average of these values was taken for discussion.

In order to do a more realistic commercial viability assessment of the system, new parameters were introduced by us. These are specific enhancement in compressive and flexural strengths, and specific compressive and flexural strengths. The specific enhancement in compressive and flexural strengths as a function of low pressure ITC method time as well as

specific compressive and flexural strengths as a function of time till the end of each method were computed as follows:

$$\sigma_c = \frac{c_d - c_i}{t_d - t_i} \tag{13}$$

$$\sigma_f = \frac{f_d - f_i}{t_d - t_i} \tag{14}$$

$$\partial_{ci} = \frac{c_i}{t_i} \tag{15}$$

$$\partial_{cd} = \frac{c_d}{t_d} \tag{16}$$

$$\partial_{fi} = \frac{f_i}{t_i} \tag{17}$$

$$\partial_{fd} = \frac{f_d}{t_d} \tag{18}$$

where,

σ_c =   specific enhancement in compressive strength,

c_d =   compressive strength after low pressure ITC method,

c_i =   compressive strength after high pressure HP method,

t_d =   total processing time till low pressure ITC method,

t_i =   total processing time till high pressure HP method,

σ_f =   specific enhancement in flexural strength,

f_d =   flexural strength after low pressure ITC method,

f_i =   flexural strength after high pressure HP method,

∂_{ci} =   specific compressive strength after high pressure HP method,

∂_{cd} =   specific compressive strength after low pressure ITC method,

∂_{fi} =   specific flexural strength after high pressure HP method,

∂_{fd} =   specific flexural strength after low pressure ITC method.

Permeability measurement

The helium gas permeability of thin flat plates fabricated out of the compact was checked through indigenously designed and developed permeability tester [35]. The equation used for the purpose is described as follows:

$$\varphi = \frac{V_p}{a.t} \tag{19}$$

where,

φ =   permeability in $\dfrac{cm^3}{cm^2.s}$ for thickness t_h and pressure P at constant temperature,

V_p =   volume of the gas permeates during test (cm^3),

a =   area of the sample under test (cm^2),

t =   time of the test (s).

Results and discussion

During high pressure HP method, the stabilized IMP (SP), which was used as PMP melts between 220-270°C and slowly flows into the gap between reinforcement under the application of hot-pressing pressure. At around 400°C, spheres are formed in the molten SP which exhibit highly oriented structure. This ordered structure is known as mesophase. The mesophase comprises polynuclear

aromatic species, which are stacked in parallel arrays to form a discotic-nematic liquid crystal system. Under prolonged heating, the spheres collide and coalesce to form larger regions of extended order until whole liquid is transformed into the anisotropic phase which subsequently solidifies to form carbon at around 500-600°C. During this period, thermal decomposition and polymer condensation reactions occur, which lead to cross linking of carbon atoms with the liberation of hetero atoms like H, N, O, and S in the form of H_2O, CO_2, CO, CH_4, N_2 and SO_2 gases **[36-38]**. The liberation rate of these hetro-atoms is very crucial in giving a flawless composite system. Hence, it was studied during high pressure HP method in a wide range and the consequence of it on coupling with low pressure ITC method was checked and discussed in subsequent sections.
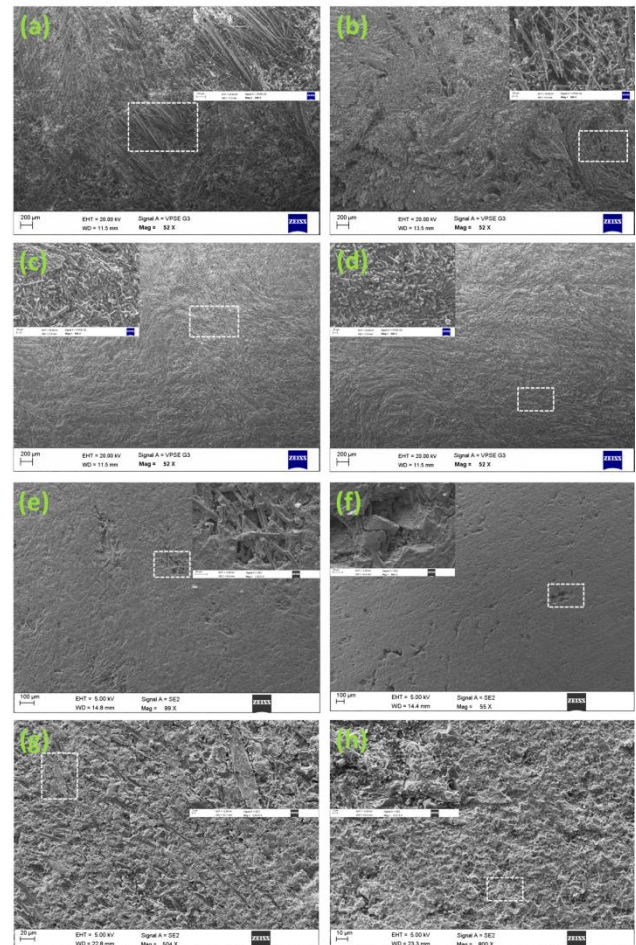
Fig. 1. SEM micrographs after primary method; (a) $HR_{0.5}$, (b) $HR_{0.3}$, (c) $HR_{0.2}$, (d) $HR_{0.1}$ and FESEM micrographs after secondary method; (e) $HR_{0.5}$, (f) $HR_{0.3}$, (g) $HR_{0.2}$, (h) $HR_{0.1}$.

Morphology

The compacts $HR_{3.3}$ and $HR_{1.0}$ upon visual inspection were found with puff like integrity and several cracks after high pressure HP method. Therefore, they were not taken up for further processing. However, compacts $HR_{0.5}$, $HR_{0.3}$, $HR_{0.2}$ and $HR_{0.1}$ were found with good self-integrity and further studies were continued with them. **Fig. 1** shows SEM micrographs of compacts $HR_{0.5}$, $HR_{0.3}$, $HR_{0.2}$ and $HR_{0.1}$ after primary method and FESEM

micrographs after coupling with secondary method. The influence of heating rate, as seen from **Fig. 1** is prominent on the microstructures. Lower heating rates seem to be more favorable in giving intact compacts with fine microstructure. The reason might be smooth liberation of hetro-atoms at lower heating rates. More specifically, the amount per unit time for higher heating rate is quite higher which would have given undesirable stresses on the matrix and reinforcement interface and the same is visible from **Fig. 1a to 1d**. Further, it can be seen that the microstructure of the compacts **(Fig. 1e to 1h)** has changed significantly upon coupling with secondary method. However, the major change occurred in the microstructure of compacts $HR_{0.5}$ and $HR_{0.3}$. The loose carbon fiber filaments seen in these compacts prior to coupling got intact after coupling. However, few spots of porosity are visible. The zoomed micrograph of these spots shows the presence of gap between filaments. It can be understood from zoomed micrograph that the necessity of further densification prevail. These porosity spot may disappear upon further densification. But, for one to one comparison the number of cycles during secondary method was kept constant for all compacts. Further densification may lead to uneven distribution of matrix and reinforcement which may cause localized failure due to presence of single constituent (either reinforcement or matrix). Further, it can be seen from **Fig. 1,** the micrographs of compacts $HR_{0.2}$ and $HR_{0.1}$ which were fine prior to coupling become finer after coupling. Additionally, the major change in these compacts would be seen in the permeability which is discussed in subsequent sections.

Density

Fig. 2 shows the variation of the density with processing stages. From **Fig. 2,** it can be seen that the density obtained during different stages of high pressure HP method has strong dependency on the parameters employed.
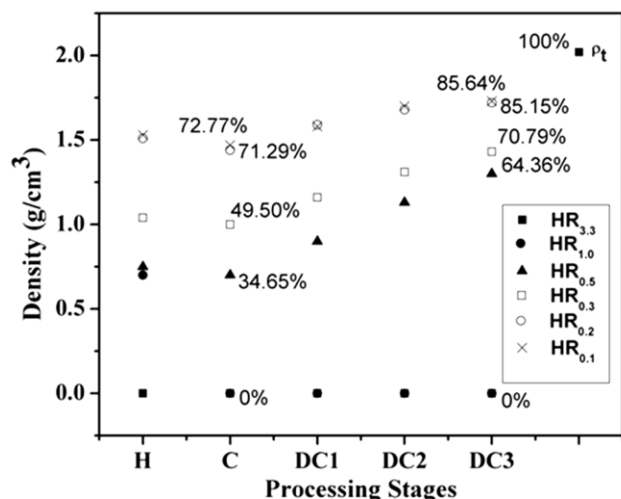
Fig. 2. Influence of processing stages on density (theoretical density: 2.02 g/cm³) for different heating rates.

The density increases as the heating rate decreases. Basically, carbon yield of the matrix precursor is one of

the factors influencing the end density and the carbon yield in turn depends upon the residence time. Lower the heating rate; higher the residence time. As a consequence of it, secondary cracking of gaseous products takes place **[33]** which increases the carbon yield. The density, as depicted in **Fig. 2,** has been increased significantly as a result of coupling with secondary low pressure ITC method. This has happened due to percolation of SMP deep into the pores which were formed during high pressure HP method. Liquid phenolic resin which was used as SMP for deriving SCM was thermoset within the pores by the application of temperature. It was then converted into SCM by carbonizing the compacts at 1050°C. Due to this carbonization, again some pores were created which were filled in subsequent cycles **[39-40]**. **Fig. 3** shows the schematic of pore filling and deposition of carbon matrix from SMP within the pores. Further, from slope, it can be seen that the rate at which density increases during first and second cycles is almost similar for all the compacts. Further, during 3rd cycle, the rate remains almost same for compacts $HR_{0.3}$ and $HR_{0.5}$. But the rate drastically falls for compacts $HR_{0.2}$ and $HR_{0.1}$.
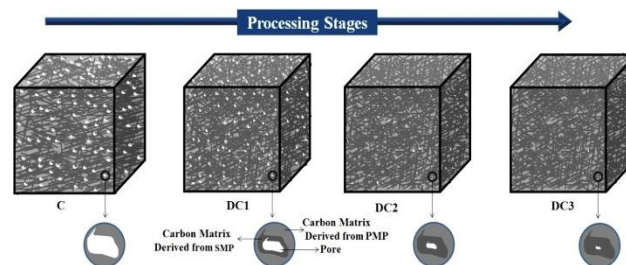
Fig. 3. Schematic of pore filling mechanism during low pressure ITC method.

Porosity

The porosity is one of the critical parameter deciding the engineering utility of a material. It is so critical in the areas of fuel cell and transport pipes that it may restrict the utility of the particular material if not addressed properly. In these areas of application, the close porosity may be allowed but open porosity restricts their usage because it increases the permeability. The total porosity of the compacts was calculated through the empirical equations reported in the literature **[33]** and the same was compared with the experimentally obtained porosity. Theoretically calculated and experimentally obtained porosities after each cycle of secondary method are inferred in **Fig. 4.** From **Fig. 4,** it can be seen that the final porosity of the compacts $HR_{0.1}$ and $HR_{0.2}$ after coupling was reduced to almost half of their initial porosity. However, the porosity left for compacts $HR_{0.3}$ and $HR_{0.5}$ after similar cycles was more than 50 % of their initial porosity. It shows the importance of the conditions employed during primary method. Further, the lag between the theoretical porosity and the experimentally obtained one after each cycle of secondary method for all heating rates can be seen. However, this lag was less in initial cycles and as number of cycles increased the lag started widening. It can be attributed to the following two happenings: 1. Initially, most of the pores might be open allowing more impregnation of SMP resulting in more

carbon matrix per unit area or volume, 2. In later stages of processing, a fraction of pores might have become closed. As a consequence of it, the production of carbon matrix per unit area or volume would have fallen. Due to this, inspite of repeated cycles of low pressure ITC method, the experimentally obtained porosity wouldn't have followed the theoretically calculated porosity.
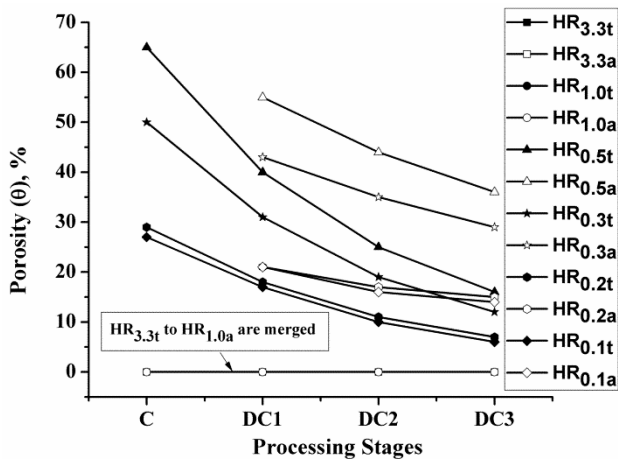

Fig. 4. Porosity variation for different hot-pressing rates during low pressure ITC method.

Mechanical properties

Mechanical properties apart from many other requirements are the key to decide the engineering utility of a material. The mechanical properties with competent processing time and cost become more crucial in the competitive world. **Table 1** shows the mechanical properties of the compacts. From **Table 1**, it can be seen that the flexural and compressive strengths of the samples have increased enormously after coupling with low pressure ITC method. It shows the importance of coupling to get a suitable composite system.

Table 1. Variation of mechanical properties with process coupling.

Compact No.	After high pressure HP method					After low pressure ITC method						
	t_i h	f_i MPa	c_i MP P a	∂_{fi} MPa /h	∂_{ci} MPa/ h	t_d h	f_d M Pa	c_d MP a	∂_{fd} MPa/ h	∂_{cd} MPa /h	σ_f MPa /h	σ_c MPa /h
$HR_{3.3}$	39	--	--	--	--	112	--	--	--	--	--	--
$HR_{1.0}$	46	--	--	--	--	119	--	--	--	--	--	--
$HR_{0.5}$	57	17	25	0.29	0.44	130	41	93	0.32	0.72	0.33	0.93
$HR_{0.3}$	70	31	48	0.44	0.69	143	52	115	0.36	0.80	0.29	0.92
$HR_{0.2}$	90	60	129	0.67	1.43	163	77	161	0.47	0.99	0.23	0.44
$HR_{0.1}$	141	63	141	0.45	1	214	81	195	0.38	0.91	0.25	0.74

The huge gap in the end properties of the compacts obtained after coupling shows the criticality of the processing conditions employed during primary HP method. The commercial assessment was done by co-relating the end properties with processing time. As a result of this co-relation, new denominations were derived first time. The values of these denominations are grouped in **Table 1**. From **Table 1,** it can be seen that the specific enhancement in strengths of compacts $HR_{0.5}$ and $HR_{0.3}$ is higher than those of $HR_{0.2}$ and $HR_{0.1}$. However, the values of flexural and compressive strengths after coupling are more for compacts $HR_{0.2}$ and $HR_{0.1}$ than those of $HR_{0.5}$ and $HR_{0.3}$. It shows the rate of increase in the mechanical properties is higher for the compacts processed @ higher

heating rate than those processed @ lower rates. Though specific enhancement is higher for compacts processed @ higher rates, the end properties are not so lucrative. Hence, some more parameters like specific strengths need to be devised to assess the viability w.r.t. end properties and the processing time. Accordingly, specific strengths after primary and secondary methods were calculated. From the specific strengths of the compacts, it can be easily concluded that the compact $HR_{0.2}$ has upper hand among all. **Fig. 5** shows the variation of hardness with processing cycles. From **Fig. 5**, it can be observed that the hardness after primary method is lower than that obtained after secondary method. The main cause behind this lies in the fact that the carbon matrix derived from SMP is glassy whereas the one which is derived from PMP is graphitic in nature. The hardness of glassy matrix is generally higher than that of graphitic matrix. As a result of coupling, the carbon matrix derived from SMP was formed in the compacts which resulted in the enhancement of the hardness. Further, the standard deviation in the hardness of the compacts $HR_{0.5}$ and $HR_{0.3}$ is very high than that of compacts $HR_{0.2}$ and $HR_{0.1}$. It would have happened due to the non-uniform distribution of matrix and reinforcement in the case of compacts processed at higher heating rates due to pre-existing holes, cracks, loose fiber ends, etc.
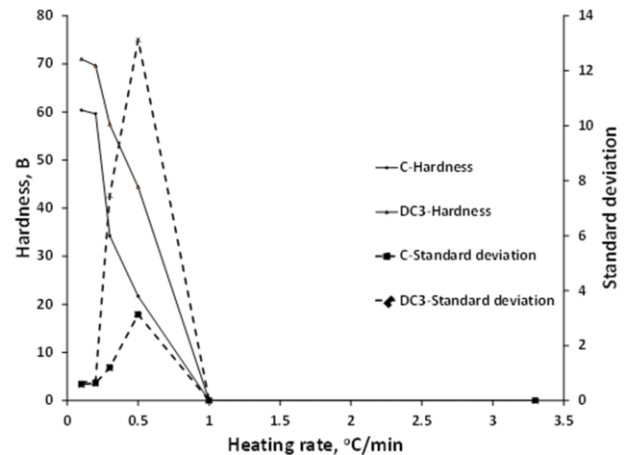

Fig. 5 Hardness variation with primary and secondary methods for different hot-pressing rates.

Fracture behavior

The fracture surface evaluation in the case of composites not only infers the qualitative information about the bond strength of reinforcement and matrix but also tells about the failure behavior. Hence, to evaluate the bond strength and fracture behavior of present system, the SEM micrographs of fracture surfaces after flexural strength were taken. The consolidated form of SEM micrographs is shown in **Fig. 6**. The cavities in the matrix left behind by fiber filaments can be seen for compacts $HR_{0.5}$ and $HR_{0.3}$. The carbon fiber ends are rarely seen coming out of the bulk matrix surface for these compacts. However, the carbon fiber ends are seen for compact $HR_{0.2}$ and the cavities are almost absent in this. Further, these cavities and fiber ends get disappeared from compact $HR_{0.1}$ and presence of filament shearing comes into picture. In

nutshell, the SEM micrographs of these compacts infer the presence of weak bond, strong bond and very strong bond for compacts $HR_{0.5}$ & $HR_{0.3}$, $HR_{0.2}$ and $HR_{0.1}$, respectively. The point of initiation of failure in composite system is an important input to determine whether failure is brittle or non-brittle. The initiation of failure at matrix, the continuous phase of the composite system, is desirable to get non-brittle failure. However, if the bond between matrix and reinforcement is either very strong or very weak, the failure even at matrix doesn't contribute much in non-brittle failure, and it leads to brittle failure. The failure at matrix depends upon several parameters like processing conditions, source of derivation, etc. The important dependency area of matrix failure as shown by Evans and co-workers [41], is processing condition under which matrix is derived. The failure propagation in a composite system takes place from one constituent to other. Generally, the initiation of failure takes place at matrix and as soon as the matrix fails due to crack generation, the applied load gets transferred to reinforcement through a shear stress mode at the reinforcement interface [42]. From **Fig. 6**, it can be seen that the failure behavior shown by compacts $HR_{0.5}$ & $HR_{0.3}$ seems to be brittle due to weak bond strength between matrix and reinforcement. No trace of crack generation at matrix is seen. The failure seems to be taken place at fiber and matrix interface. However, the failure in the case of compacts $HR_{0.2}$ & $HR_{0.1}$ seems to be non-brittle due to presence of cracks within the matrix.
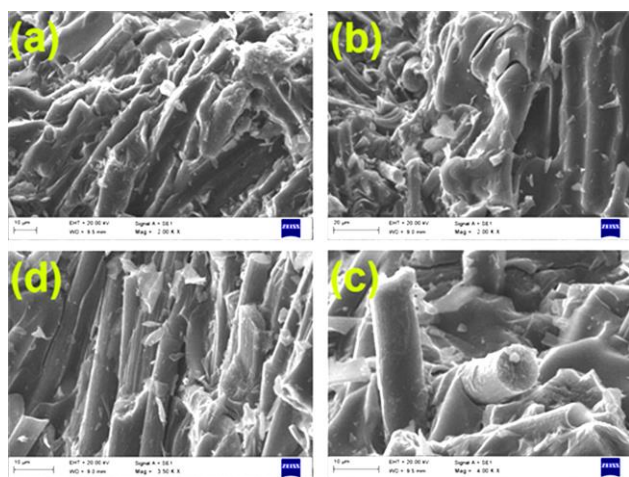

Fig. 6. SEM micrographs of fracture surface after three point bending test; a) $HR_{0.5}$, b) $HR_{0.3}$, c) $HR_{0.2}$, d) $HR_{0.1}$.

The failure initiation, as evident from **Fig. 6,** seems to take place at matrix from micro-cracking of the matrix, and ends with sharp breakage of carbon fibers and shearing of carbon fibers for compacts $HR_{0.2}$ and $HR_{0.1}$, respectively. The fiber breakage after pulling in the case of compact $HR_{0.2}$ and fiber shearing without pulling in the case of compact $HR_{0.1}$ shows that the bond of compact $HR_{0.2}$ is comparatively weaker and weaker bond helps in de-bonding at reinforcement and matrix interface which is desirable as reported in literature [42] for the activation of energy absorbing mechanisms such as crack deflection, crack bridging, fiber fracture and finally fiber pullout, which impedes crack propagation in the composite at the

reinforcement/matrix interface, and ultimately results in a non-brittle behavior. Based on this hypothesis, the failure behavior shown by compact $HR_{0.2}$ looks to be better than rest.

Permeability

The validation of the impact of coupling low pressure ITC method with high pressure HP method on the utility of the material from application point of view was done by measuring the permeability (qualitative and quantitative) of the selected compacts. For measuring permeability, the specialized permeability tester was designed and developed [35]. The qualitative permeability check of selected samples (from OE-8 and OE-9) was done using the specially designed permeability tester by seeing the bubble formation in the water kept on the sample. The quantitative measurement was performed on those samples which passed the qualitative test. The schematic of the slicing of the test specimens with thickness of 1, 1.5, 2, 3, 4, and 5 mm for permeability measurement is shown in **Fig. 7**. The permeability of the compacts $HR_{0.2}$ and $HR_{0.1}$ after three densification cycles was found to just meet the specified target of commercial bipolar plate of PEM fuel cell. However, small change in the permeability of compacts $HR_{0.2}$ and $HR_{0.1}$ was observed. Further, the permeability was found to vary minutely with test specimen thickness. It can be noted that the permeability of composites changes with thickness due to thickness dependency. However, in our case same was found negligible. It shows the effectiveness of the methodology for producing a bulk C/C composite with very high degree of uniformity.
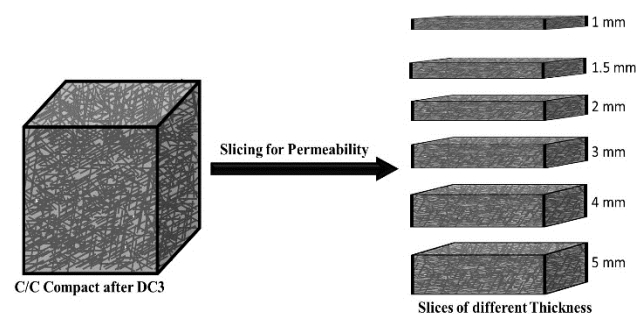

Fig. 7. Schematic of slicing of test specimens from bulk composite for permeability measurement.

Conclusion

From the campaign of experimental proceedings following conclusions can be drawn: The C/C composite with a density as high as 1.70 g/cm^3, flexural strength as high as 77 MPa and compressive strength as high as 161 MPa was successfully fabricated in a record time of 163 h by coupling the processes. The conditions employed during primary method were found very detrimental in controlling the microstructure of the composite and densification and mechanical properties thereafter. The new denominations introduced first time for the assessment of commercial viability of the composite system were found highly relevant. The C/C composite developed was found with low permeability. The
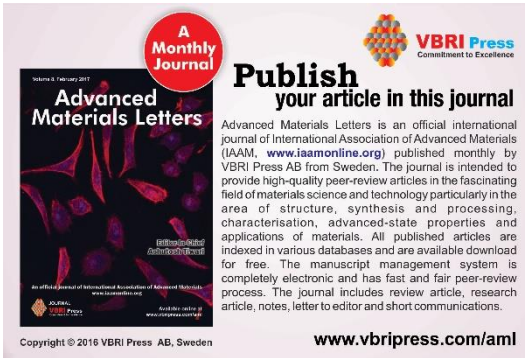
functional performance of the composite system will be done in subsequent works.

References

1. Xiong, X.; Huang, B-Y.; Li, J-H.; Xu, H-J.; *Carbon*, **2006**, *44*, 463.
2. Yudin, V.E.; Goykhman, M.Y.; Balik, K.; et al.; *Carbon*, **2002**, *40*, 1427.
3. Manocha, L.M.; Patel, M.; Manocha, S.M.; et al.; *Carbon*, **2001**, *39*, 663.
4. Liedtke, V.; Hüttinger, K.J.; *Carbon*, **1996**, *34*, 1081.
5. Vix-Guterl, C.; Shah, S.; Dentzer, J.; et al.; *Carbon*, **2001**, *39*, 673.
6. Oh, S.M.; Park, Y.D.; Lim, Y.S.; Yoon, B.I.; *Carbon*, **1993**, *31*, 391.
7. Gajiwala, H.M.; Vaidya, U.K.; Sodah, S.A.; Jeelani, S.; *Carbon*, **1998**, *36,* 903.
8. Chen, W.; Yu, Y.; Li, P.; et al.; *Compos. Sci. Technol.,* **2007**, *67*, 2261.
9. Dhakate, S.; Mathur, R.; Dhami, T.; *Carbon Lett.*, **2002**, *3*, 127.
10. Su, J-M.; Xiao, Z-C.; Liu, Y-Q.; et al.; *New Carbon Mater*., **2010**, *25*, 329.
11. Blanco, C.; Bermejo, J.; Marsh, H.; *Wear*, **1997**, 213, 1.
12. Goto, K.; Hatta, H.; Kogo, Y.; et al.; *Adv. Compos. Mater*., **2003**, *12*, 205.
13. Forster, N. H.; Rosado, L.; Brown, J. R.; Shih, W. T.; *Tribol. Trans.,* **2002**, *45*, 127.
14. Peng, L-N.; He, G-Q.; Li, J.; et al.; *Carbon*, **2012**, *50*, 1554.
15. Vignoles, G.L.; Aspa, Y.; *Compos. Sci. Technol.*, **2010**, *70*, 1303.
16. Chen, B.; Zhang, L-T.; Cheng, L-F.; Luan, X-G.; *Carbon*, **2009**, *47*, 1474.
17. Raunija, T.S.K.; Mathew, M.; Sharma, S.C.; *Bharatiya Vaigyanik evam Audyogik Anusandhan Patrika*, 2014, *22*, 87.
18. Wang, Q.; Han, X.H.; Sommers, A.; et al.; *Int. J. Refrig..*, **2012**, *35*, 7.
19. Northam, G.B.; Rivers, H.K.; *Adv. Eng. Mater.*, **2000**, *2*, 583.
20. Venugopalan, R.; Sathiyamoorthy, D.; Acharya, R.; Tyagi, A.K.; *J. Nucl. Mater.*, **2010**, *404*, 19.
21. Venugopalan, R.; Roy, M.; Thomas, S.; et al.; *J. Nucl. Mater.*, **2013**, *433*, 494.
22. Besmann, T.M.; Klett, J.W.; Henry, J.J.; et al.; *J. Electrochem. Soc.*, **2000**, *147*, 4083.
23. Raunija, T.S.K.; Mathew, M.; Sharma, S.C.; *Powder Technol.*, **2014**, *267*, 273.
24. Marković, V.; Marinković, S.; *Carbon*, **1980**, *18*, 329.
25. Manocha, L.M.; Bhatt, H.; Manocha, S.M.; *Carbon*, **1996**, *34*, 841.
26. Ko, T-H.; Jaw, J-J.; Chen, Y-C.; *Polym. Compos.*, **1995**, *16*, 522.
27. Ko, T-H.; Kuo, W-S.; Chang Y-H.; *Polym. Compos.*, **2000**, *21*, 745.
28. Raunija, T.S.K.; Babu, S.; *AIP Conf. Proc.*, **2013**, *1538*, 168.
29. Raunija, T.S.K.; Babu, S.; Wesley, C.S.; *Indian Patent*, **2012**, App. 1713/CHE/2012.
30. Raunija, T.S.K.; Manwatkar, S.K.; Sharma, S.C.; Verma, A.; *Carbon Lett.*, **2014**, *15*, 25.
31. Raunija, T.S.K.; *Indian J. Eng. Mater. Sci.*, **2015**, *22*, 541.
32. Raunija, T.S.K.; Sharma, S.C.; *Carbon Lett.*, **2015**, *16*, 25.
33. Rellick, G.; *Carbon*, **1990**, *28*, 589.
34. Matzinos, P.D.; Patrick, J.W.; Walker, A.; *Carbon*, **2000**, *38*, 1123.
35. Raunija, T.S.K.; Mathew, M.; Sharma, S.C.; Verma A.; *Indian Patent*, **2016**.
36. Morgan, P.; Carbon fibers and their composites, CRC PressI Llc, **2005**.
37. Savage, G.; Carbon-carbon composites, Springer, **1993**.
38. Carrington, A.; Smith, I.C.P.; *Mol. Phys.*, **1965**, *9*, 137.
39. Wu, X.; Luo, R.; Ni, Y.; Xiang, Q.; *Composites Part A*, **2009**, *40*, 225.
40. Kuo, H.H.; Lin, J.H.C.; Ju, C.P.; *Carbon*, **2005**, *43*, 229.
41. Evans, A.G.; *Acta Metall.*, **1989**, *37*, 2567.
42. Odeshi, A.G.; Mucha, H.; Wielage, B.; *Carbon*, **2006**, *44*, 1994.